Journal of Macromolecular Science, Part A
Publication details, including instructions for authors and subscription information:
http://www.informaworld.com/smpp/title~content=t713597274

How to Estimate the Strength of Plastic Structural Components

G. Menges[a]; E. Alf[a]
[a] Institut fur Kunststoffverarbeitung an der Rheinisch-Westfalischen Technischen Hochschule, Aachen, Germany

To cite this Article Menges, G. and Alf, E.(1972) 'How to Estimate the Strength of Plastic Structural Components', Journal of Macromolecular Science, Part A, 6: 7, 1251 — 1265
To link to this Article: DOI: 10.1080/10601327208056894
URL: http://dx.doi.org/10.1080/10601327208056894

J. MACROMOL. SCI.—CHEM., A6(7), pp. 1251-1265 (1972)

How to Estimate the Strength of Plastic Structural Components

G. MENGES and E. ALF

Institut für Kunststoffverarbeitung an der Rheinisch-Westfälischen
Technischen Hochschule
Aachen, Germany

ABSTRACT

A simple and safe method for calculating permissible stress for plastic structures by using limits of permissible deformation are presented. When these deformation limits are exceeded, crazes are formed in amorphous resins, and microcracks are formed in semicrystalline thermoplastics and reinforced resins. The deformation limits are characteristic of the materials data but independent of time, temperature, and the stress distribution.

INTRODUCTION

Plastic materials are to a considerable extent used for articles produced in large numbers. Determination of the loading capacity is therefore replaced by an estimation-like method since the first items produced can be tested under practice-like conditions.

Yet in order to avoid severe changes of costly tools, the designer desires help in determining adequate dimensions for the critical cross sections. Up to now he has applied the methods of a strength theory that is recommended for metals: stresses expected to occur in critical cross sections are compared with permissible values found to be characteristic for materials.

For fracture, a value K_B is derived from the tensile strength σ_B and a safety factor S_B:

$$K_B = \sigma_B/S_B$$

Likewise a calculation against excessive deformation can be made choosing a stress value from a tensile stress-strain or fatigue diagram at which a uniaxially loaded specimen reaches a certain deformation (e.g., 1%).

$$K_v = \sigma_{1\%}/S_v$$

The modulus of elasticity E determines the permissible material-specific value K_I for loads under which structures fail (e.g., in case of buckling).

$$K_I = E/S_I$$

For multiaxial loads, stresses are superposed on the base of a strength hypothesis to yield a reference stress value which is compared with known material data. This procedure has a great disadvantage for plastics: it does not take into account that stresses and the modulus of elasticity depend on time, temperature, and sometimes on the magnitude of the effective stress itself. Maldesign results from the designers inability to understand the complicated relationships which become even more intricate with anisotropic materials. Here the calculating procedure is a formidable task and out of economic relation with the requirements of practice. Therefore a new calculating method has been developed which has proved to be advantageous for predicting the loading capacity of large structures such as silos and roofing structures [1] of glass reinforced polyester and epoxide resins as well as of thermoplastic injection molded parts [2]. Such moldings, which are anisotropic thanks to their orientation and the internal stresses resulting, e.g., from cooling mechanisms, have to be carefully dimensioned, particularly because of their stress-cracking tendency. The method suggested here affords safe dimensioning avoiding stress-cracking corrosion.

MECHANICAL BEHAVIOR OF MATERIALS UNDER TENSILE LOAD

It has been observed that isotropic amorphous translucent thermoplastics exhibit flow phenomena normal to the main tensile strain. These are called crazes or fissures, and they occur once a critical deformation, e.g., by a load effective over a long time, is exceeded [3-5].

This deformation value ϵ_F tends asymptotically over time to a limiting value $\epsilon_{F\infty}$ (see Fig. 1) [6]. If the deformation is less than

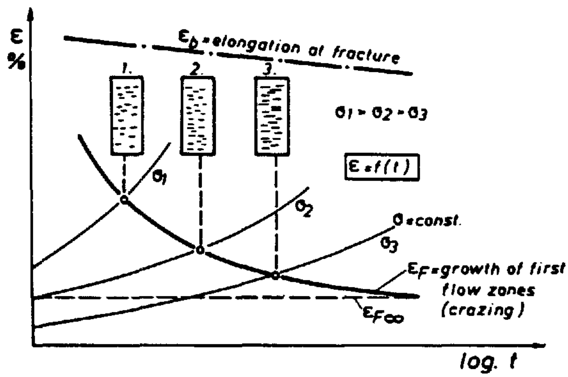

FIG. 1. Line of first onset of flow zones in the one-dimensional creep test, with schematic indication of size and position of the flow zones formed.

this value, no crazes occur and the material behaves like a pseudo-elastic body, i.e., after unloading the deformation disappears entirely within a finite time. The limiting deformation value $\epsilon_{F\infty}$ is, as long as the material state remains unchanged, independent of temperature, the geometry of the loaded part, and the kind of load (see Fig. 2), no matter whether an impact or a static long-time one- or multidimensional load is concerned, an oscillating load, or a retarding or relaxing load. Finally, $\epsilon_{F\infty}$ is independent of the stress distribution whether homogeneous or inhomogeneous. Environmental media which do not change the material state (like aqueous solutions of wetting agents) of the plastic do not change $\epsilon_{F\infty}$ because they cannot change the state of the material unless flow zones form through which the medium can penetrate rapidly and corrode via a large surface. The limiting deformation value $\epsilon_{F\infty}$ is therefore a genuine material constant. Its validity is restricted by limits given

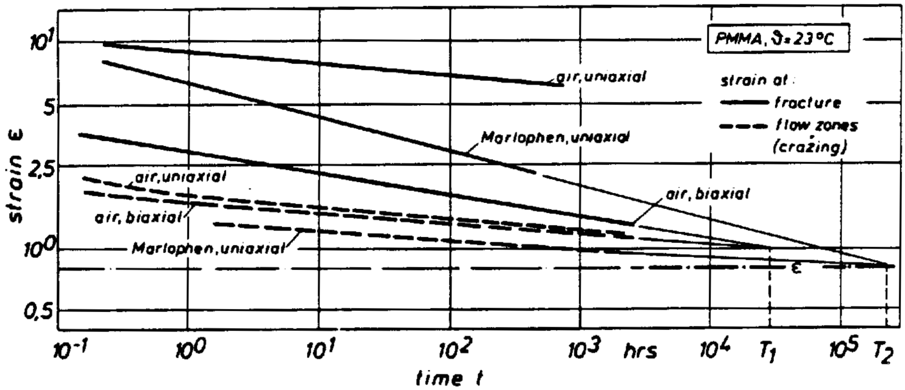

FIG. 2. Lines of first onset of flow zones ϵ_F and of elongation at fracture ϵ_B as functions of environmental influence and multidimensional load.

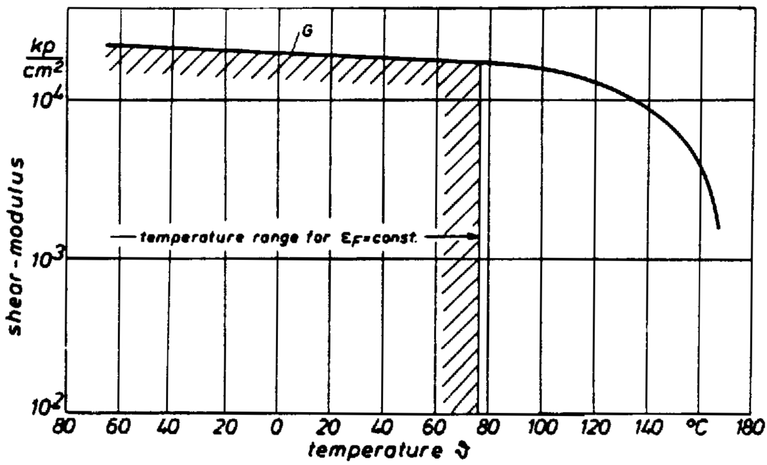

FIG. 3. Shear-modulus curve of PMMA with permissible temperature range (working temperature $\vartheta <$ softening point ϑ_{ET}) determined by means of the torsional oscillation test DIN 53 445. The mechanical fatigue limit with the change of state is shown in this shear modulus vs. temperature graph.

by material state changes over temperature which are depicted in the shear-modulus vs temperature graph (Fig. 3) [3].

Our investigations show that $\epsilon_{F\infty}$ is in the range 0.7 to 1% for many isotropic amorphous thermoplastics like polymethyl methacrylate, polycarbonate, and polyvinyl chloride. For polystyrene the deformation limit at which flow zones form lies between 0.4 and 0.5% [2]. Coloration does not usually influence these values.

Crazes in isotropic partially crystalline thermoplastics can be recognized by a milky looking structure Here the viscous behavior of the amorphous phase complicates the analysis compared to purely amorphous polymers.

Nevertheless the limiting deformation value $\epsilon_{F\infty}$ can be determined with satisfactory accuracy. It obviously lies between 1 and 2.5% deformation according to the results of tests on partially crystalline polymers. As for pseudoisotropic glass-fiber mats of reinforced polyester and epoxy resins, beyond certain limiting deformations these resins separate at the interface from those fibers which are orientated normal to the main tensile strain. Therefore a limiting deformation value $\epsilon_{F\infty}$ can be defined [1], ranging here between $\epsilon_{F\infty} = 1.2\%$ at a glass content of $\varphi = 8\%$ and $\epsilon_{F\infty} = 0.5\%$ at $\varphi = 33\%$.

FINDING THE LIMITING DEFORMATION VALUE $\epsilon_{F\infty}$

Isotropic or Pseudoisotropic Materials

The deformation values can only be determined by creep tests. At higher temperatures in the area of limiting values below ϑ_{ET} (see Fig. 3), only a few hours are needed to conduct complete creep tests. These limiting values are entered on the material-specific isochronous stress-strain diagram (Fig. 4) and enable the designer to correlate calculated stresses with the deformations. Isochronous stress-strain plots have been set up for most important polymer materials, thermoplastics as well as GRPs [7].

Inisotropic materials

Those parts with orientations introduced during the production process, e.g., thermoplastic injection molded parts, exhibit anisotropic behavior, i.e., the moldings' stress-strain behavior is load-direction dependent. Their behavior under load in the injection direction is different from that in the cross direction. These production process

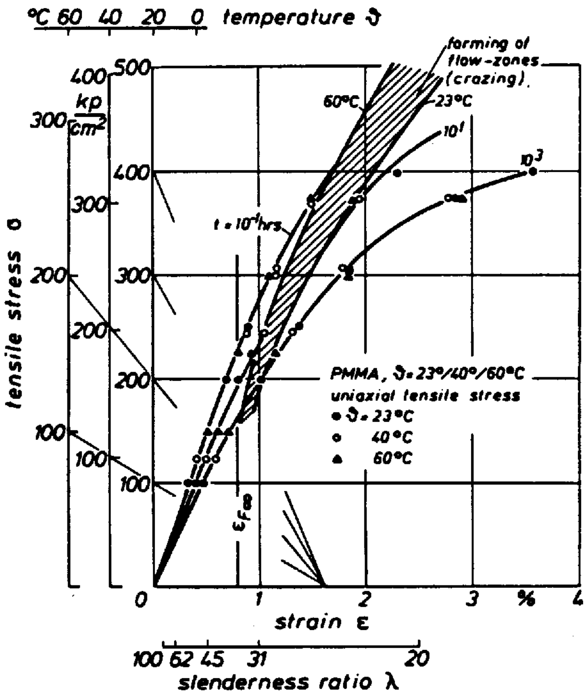

FIG. 4. Isochronous stress-strain diagram δ = f (ε,ϑ,t,λ) for various temperatures, times, and slenderness ratios.

effects are seldom desirable but, on the other hand, they are inevitable. Only for fiber-reinforced materials is anisotropic behavior desired in order to meet practice requirements. For anisotropic materials, isochronous stress-strain diagrams and the limiting deformation values $\epsilon_{F\infty}$ for the extreme directions are needed; for moldings this means parallel to the orientation and in the cross direction. Orientation does not affect the modulus of homogeneous materials such as polystyrene moldings, but does affect the limiting deformation value. This value tends to greater deformations parallel to the orientation, in the orthogonal direction it tends to lower values (Fig. 5). Orientations can be estimated from processing conditions (stock- and tool temperature, filling speed, flow distance, and wall thickness of the moldings) [2], or read from diagrams [2]. These new limits are transferred to isochronous stress-strain plots for isotropic materials. The

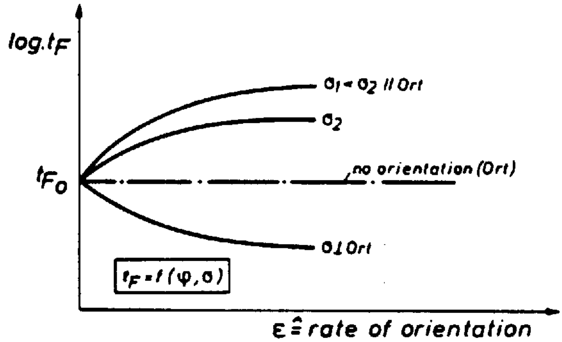

FIG. 5. Schematic graphical representation of the times after which flow zones (crazes) occur with orientated specimens under tensile-fatigue load. $Ort_{\parallel}$ = load parallel to orientation. $Ort_{\perp}$ = load normal to orientation. t_F = load duration after which flow zones (crazes) form (Fig. 6).

moduli of an inhomogeneous and anisotropic material such as glass fiber reinforced resins of a linear fortification structure differ considerably with direction so that for each of the two main fortification directions, separate isochronous stress-strain diagrams are required. The limiting deformation characteristics $\epsilon_{F\infty}$ are also different for different directions, their magnitude also being dependent on the glass fiber content or the laminate structure.

MATERIAL-SPECIFIC MECHANICAL BEHAVIOR UNDER COMPRESSIVE STRESS (STABILITY BEHAVIOR)

Investigations [8] have made it clear that stability behavior (not only of plastics) is a function of a certain compression value. The critical compression value ϵ_K for all materials at which unstable yielding and often failure occurs is determined by structure geometry and clamping conditions. The relationship can be formulated as

$$\epsilon_K = \pi^2/\lambda^2 \qquad \text{(Figs. 7 and 8)}$$

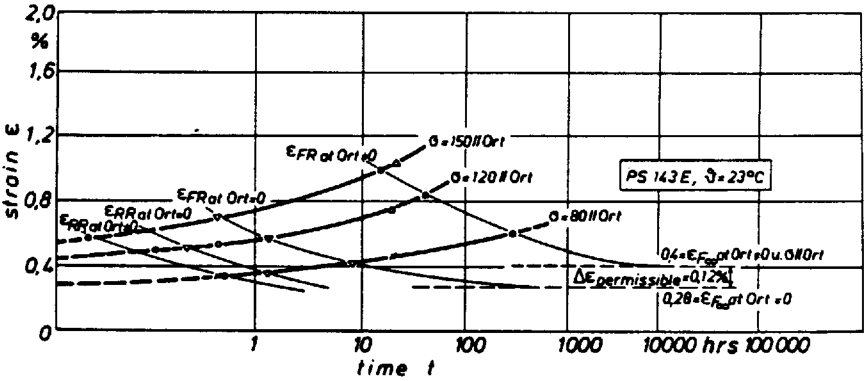

FIG. 6. Flow deformation values ϵ_F for various critical sections of injection mouldings. Ort = orientation.

where ϵ_K is the critical compression and λ the ratio of slenderness. By means of this formula all the available knowledge about stability behavior can be transferred from any material to plastics. For structure geometries, such as polyethylene beer crates which inhibit a mathematical solution, the critical compression values can be obtained from creep tests of relatively short duration (about 10 hr) which have to be conducted for each geometry. For such monocoque structures for which solutions are available, the ratios of slenderness are given (Table 1). Therefore it is sufficient to introduce an axis for the ratio of slenderness parallel to the strain coordinate of an isochronous stress-strain diagram for a certain material (see Fig. 4). To calculate the stability, first determine λ for a given geometry, enter it on the isochronous stress-strain graph, and pick out the stress at which failure occurs after a certain working time. For anisotropic materials that show direction-dependent elastic behavior (modulus of elasticity) one needs isochronous stress-strain curves for each direction to which the coordinate has to be added parallel to the strain scale. For this the assumption has to be made that the isochronous stress-strain diagram or the moduli, respectively, are the same for compressive and tensile load. This assumption, as was shown, is justified for relatively low deformations occurring with all laminates in connection with instability.

MULTIAXIAL LOAD

Isotropic Materials

Thus far it has been emphasized that critical deformations in any direction in a structure should not be exceeded. These deformations

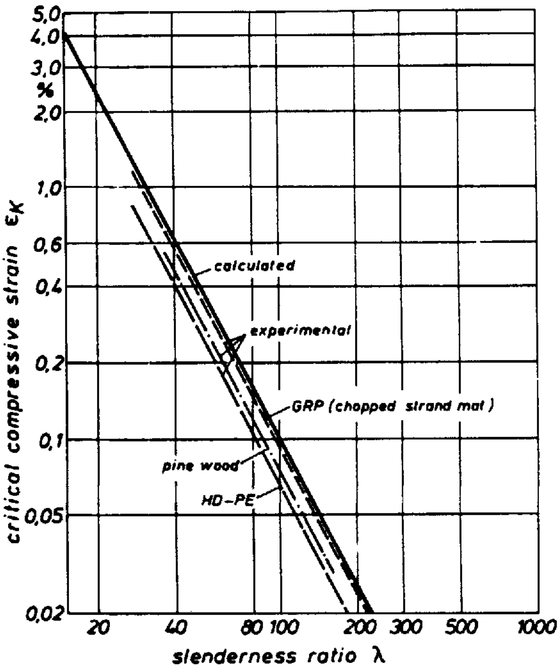

FIG. 7. Buckling compression ϵ_K as a function of the slenderness ratio for materials, metals, PE, glass mat reinforced polyester resin, and pine wood.

are generally (except for monoaxial test specimens) caused by stresses effective in various directions. Contrary to the usual practice, it is helpful to calculate the effective main deformations $\epsilon_{i\ eff}$ of a structure under a three-dimensional load σ_i with Hooke's law:

$$\epsilon_{1\ eff} = \epsilon_{\sigma_1} - \mu\epsilon_{\sigma_2} - \mu\epsilon_{\sigma_3}$$

$$\epsilon_{2\ eff} = \epsilon_{\sigma_2} - \mu\epsilon_{\sigma_3} - \mu\epsilon_{\sigma_1}$$

$$\epsilon_{3\ eff} = \epsilon_{\sigma_3} - \mu\epsilon_{\sigma_3} - \mu\epsilon_{\sigma_1}$$

This shows that the main deformations $\epsilon_{i\ eff}$ of a structure can be calculated from the deformations ϵ_{σ_i} of one-dimensionally loaded

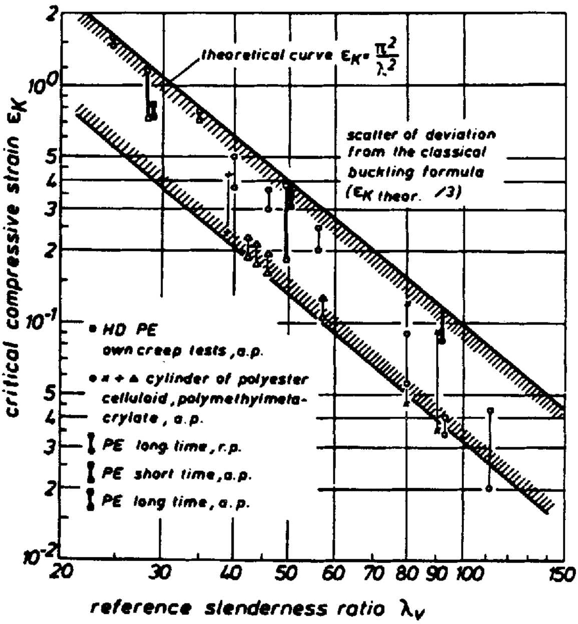

FIG. 8. Buckling of cylinders (shells) of various materials under axial pressure (a.p.) and radial pressure (r.p.).

specimen of the same material. In other words, for isotropic materials the isochronous stress-strain diagram provides, for any loading condition, the necessary material data as functions obtained from creep tests. The conditions for the permissible load are then:

$$\epsilon_{\text{eff i max}} < \epsilon_{F\infty} \qquad \text{for tensile strain}$$

and

$$\epsilon_{\text{eff i max}} < -\epsilon_k / S_K \qquad \text{for compression}$$

Safety coefficients normally are not required for positive deformations or have only small values ($S < 1,5$) since the limiting deformation values $\epsilon_{F\infty}$ clearly lie below the rupture strain ϵ_B: $\epsilon_{F\infty} < \epsilon_B$.

For compression, however, factors have to be introduced whose

TABLE 1. Equivalent Slenderness Ratios of Various Structural Shapes

loading case	figure	classic law for buckling	critical buckling stress	equivalent slenderness ratio	author
Buckling of a bar under axial load	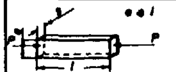	$P_{cr} = \frac{\pi^2 E I}{l_e^2}$	$\sigma_{cr} = \frac{E \pi^2}{12} \frac{s^2}{l_e^2}$	$\lambda = \frac{l_e}{s}\sqrt{12}$	Euler
Buckling of a plate under axial load	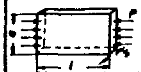	—	$\sigma_{cr} = \frac{E \pi^2}{12(1-\mu^2)} \frac{s^2}{l^2} k_l$	$\lambda_v = \frac{l_e}{s}\sqrt{\frac{12(1-\mu^2)}{k_l}}$	Pfluger s 396
Buckling of a spherical shell under radial pressure		$p_{cr} = \frac{2}{\sqrt{3(1-\mu^2)}} E (\frac{s}{r})^2$	$\sigma_{cr} = \frac{E}{\sqrt{3(1-\mu^2)}} (\frac{s}{r})$	$\lambda_v = \pi \sqrt{\frac{r}{s}} \sqrt[4]{3(1-\mu^2)}$	Zoelly + Karman
Buckling, of a short cylindrical shell under radial pressure	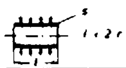	$p_{cr} = 0{,}92\ E \frac{r}{l} (\frac{s}{r})^{5/2}$	$\sigma_{cr} = 0{,}92 \cdot E \cdot \frac{r}{l} \sqrt{(\frac{s}{r})^3}$	$\lambda_v = \frac{\pi}{0{,}92} \sqrt{\frac{l}{r}} \cdot \sqrt{(\frac{r}{s})^3}$	Ebner
Buckling of a conical shell under axial pressure	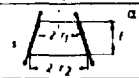	$p_{cr} = 0{,}8\ 0{,}92 \cdot E \frac{\rho}{l} (\frac{s}{\rho})^{5/2}$	$\sigma_{cr} =$ $0{,}8\ 0{,}92\ E \frac{s}{l} \sqrt{(\frac{s}{\rho})^3}$	$\lambda_v = \frac{\pi}{0{,}8\ 0{,}92} \sqrt{\frac{l}{\rho}} \sqrt[4]{(\frac{\rho}{s})^3}$ $\rho = \frac{(r_1 + r_2)}{2 \cos \alpha}$	Pfluger
Buckling of a circular cylinder under radial pressure	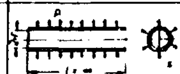	$p_{cr} = \frac{E}{4(1-\mu^2)} (\frac{s}{r})^3$	$\sigma_{cr} = \frac{E}{4(1-\mu^2)} (\frac{s}{r})^2$	$\lambda_v = 2\pi \frac{r}{s} \sqrt{1-\mu^2}$ *	v Mises
Buckling of a circular cylinder under axial pressure	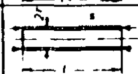	—	$\sigma_{cr} = \frac{s E}{r \sqrt{3(1-\mu^2)}}$	$\lambda_v = \pi \sqrt{\frac{r}{s}} \cdot \sqrt[4]{3(1-\mu^2)}$	Bresse
Buckling of a circular cylinder with frames under radial pressure	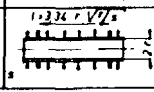	$p_{cr} = 0{,}92\ E \frac{r}{l} (\frac{s}{r})^{5/2}$	—	$\lambda_v = \frac{\pi}{0{,}92} \sqrt{\frac{l}{r}} \sqrt[4]{(\frac{r}{s})^3}$	v.Windenburg

Poisson's ratio amounts within the deformation considered in this table $\mu = 0{,}3$

* The relation $\frac{r}{s}$ in notet for tubes of HD-PE inaccordance to DIN 8074 to

$$\frac{r}{s} = \frac{\sigma_{p.m.}}{p_{no}} = \frac{50 kp/cm^2}{p_{no}}$$

hence it follows

$$\lambda_v = 2\pi \frac{\sigma_{p.m.}}{p_{no}} \sqrt{1-\mu^2}$$

magnitude is based on the risk of failure equalling those factors used for direct calculation of the stresses, i.e., S_K 1.5 -3. The great advantage of this method is the simple access to the permissible deformation data which are independent of environmental conditions. Further the designer's work is facilitated a great deal since he can operate with reliable material data independent of the structure shape. This method allows safe dimensioning by eliminating stress-corrosion, as our own investigations and work of others have proved [9, 10].

Moldings of Inisotropic Material Structure

Injection-Molded Parts with Orientations

Since stress-crack corrosion plays a vital role at critical cross sections, determination of the loading capacity of molded parts must account for this. Such cross sections are in the vicinity of the sprue and in those areas where rapid cooling down is effective, e.g., the outer zones from which heat can be effectively extracted in three directions simultaneously. Here orientations orthogonal to the molding's contour which was positioned in the flow direction are frozen in. In order to obtaining the strain values (shown in Fig. 9) it is advisable

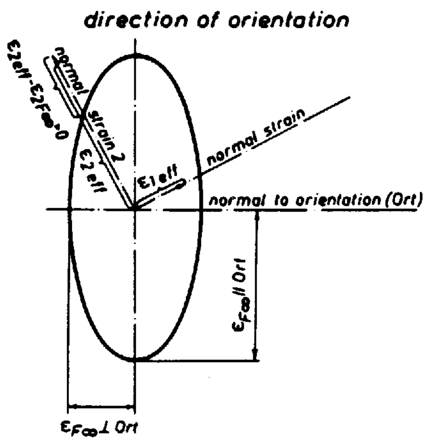

FIG. 9. Estimation of the risk of stress cracking for an injection molding with inisotropic strength properties using a polar diagram of the limiting flow deformations. $\epsilon_{F\infty}{}^{\parallel}$ = limiting flow deformation parallel to orientation. $\epsilon_{F\infty}{}^{\perp}$ = limiting flow deformation normal to orientation. $\epsilon_{1,2\ eff}$ = effective strains (tensile) at critical cross section of a molding.

to set up a polar diagram of the limiting flow deformation. The values of the limiting flow deformations in orientation direction: $\epsilon_{F\infty}^{\parallel}$ and in cross direction $\epsilon_{F\infty}^{\perp}$ are entered in the diagram as shown in Fig. 9. The four points so obtained permit the drawing of a polar diagram. The effective deformations $\epsilon_{i\ eff}$ occurring in practice are calculated as described above and are introduced according to their magnitude and direction into the graph.

One does not have to care about stress-cracking as long as the effective tensile strains are within the flow deformation limits: $\epsilon_{F\infty}^{\parallel}$, $\epsilon_{F\infty}^{\perp}$. This is a quick procedure for predicting stress-cracking behavior under practice load conditions.

Structural Components Inisotropically Reinforced with Fibers [11]

The behavior of such structures varies significantly with varying direction, poisson's ratio μ, as well as the modulus of elasticity E, and the limiting flow deformation $\epsilon_{F\infty}$ which is accounted for by the following relationships:

$$\epsilon_{1\ eff} = \frac{1}{E_1}\sigma_1 - \frac{\mu_2}{E_2}\sigma_2 - \frac{\mu_3}{E_3}\sigma_3$$

$$\epsilon_{2\ eff} = \frac{1}{E_2}\sigma_2 - \frac{\mu_3}{E_3}\sigma_3 - \frac{\mu_1}{E_1}\sigma_1$$

$$\epsilon_{3\ eff} = \frac{1}{E_3}\sigma_3 - \frac{\mu_1}{E_1}\sigma_1 - \frac{\mu_2}{E_2}\sigma_2$$

Substituting Δ_1 for σ_1/E_1, Δ_2 for σ_2/E_2, and Δ_3 for σ_3/E_3 is helpful because Δ values can be obtained directly, i.e., without computing, from creep or isochronous stress-strain graphs. Direction-specific Poisson's ratios μ_i are calculable; furthermore, publications (e.g., Ref. 12) containing these data are available. However, the supply with such creep- or stress-strain curves is still incomplete. The method introduced here needs some critical examination. Similar to the cases described above, the effective deformation in each direction occurring under practice load has to be below the critical compression ratio.

Shear Stresses

Experiments [3] have shown that shear stresses as biaxial load have to be divided into tensile and compressive components under an angle of 45%. That is why the tensile stress component is generally the more critical one leading to flow zones, stress cracking, or separation of the resin from the fibers in GRP once the permissible deformation is exceeded. Thin-walled parts tend to buckle due to the effective compressive stress component. By and large, the computing procedure is much the same as already outlined above, i.e., deformations resulting from additional stresses are to be superposed to the deformations caused by shear stress in order to determine the effective deformations in the main directions. These again have to be within the according limits: $< (\epsilon_{F\infty})$.

Oscillating Load

It has already been mentioned that in the case of an oscillating load, flow zones form at exactly the same deformation limits as are found for static load, i.e., as soon as the net deformation (static and dynamic) exceeds the critical deformation.

However, there is one effect that has to be paid attention because it must be accounted for in the stress-strain calculating procedure: the specimen temperature is elevated because a considerable amount of the kinetic energy is dissipated as heat [13].

ACKNOWLEDGMENT

The author thanks Mr. Leibfried, Mr. Schmidt, and Mr. Roskothen for their collaboration; also Mr. Kosel who translated the paper.

REFERENCES

[1] E. Dolfen, Dissertation, Technische Hochschule, Aachen, 1969.
[2] D. Leibfried, Dissertation, Technische Hochschule, Aachen, 1970.
[3] H. Schmidt, Dissertation, Technische Hochschule, Aachen, 1970.
[4] G. Menges and H. Schmidt, Plastics Polym., 38(2), 13-19 (1970).
[5] R. P. Kambour, Polymer, 5, 143-155 (1964).
[6] G. Menges and H. Schmidt, Kunststoffe, 57, 885-890 (1967).
[7] O. Schwarz, Dissertation, Technische Hochschule, Aachen, 1968.
[8] G. Menges and E. Gaube, Mod. Plastics, 46(7), 96-110 (1969).
[9] G. Menges, H. Schmidt, and H. Berg, Kunststoffe demnächst.

[10] G. A. Bemier and R. P. Kambour, Macromolecules, 1 (5), 393-400 (1968).
[11] G. Menges, H. J. Roskothen, and P. Empt, Kunststoffe, 60, 12 (1970).
[12] A. Puck, Kunststoffe, 58, 886-893 (1968).
[13] G. Menges and E. Alf, Plastverarbeiter, 21, VIII, 1-6 (1970).

Received for Publication September 9, 1971